Progress of Theoretical Physics, Vol. 60, No. 2, August 1978

Gravothermal Catastrophe of Finite Amplitude

Izumi HACHISU, Yoshikazu NAKADA,* Ken'ichi NOMOTO**
and Daiichiro SUGIMOTO

Department of Earth Science and Astronomy
College of General Education, University of Tokyo
Komaba Meguro, Tokyo 153
**Department of Astronomy, University of Tokyo, Tokyo 113*
***Department of Physics, Ibaraki University, Mito 310*

(Received February 10, 1978)

Development of the gravothermal catastrophe is followed numerically for self-gravitating *gas system* enclosed by an adiabatic wall, which is isothermal in the initial state. It is found that the final fate of the catastrophe is in two ways depending on the initial perturbations. When the initial perturbation produces a temperature distribution decreasing outward, the contraction proceeds in the central region and the central density increases unlimitedly, as the heat flows outward. When the initial temperature distribution is increasing outward, on the other hand, the central region expands as the heat flows into the central region. Then the density contrast is reduced and finally the system reaches another isothermal configuration with the same energy but with a lower density contrast and a higher entropy. This final configuration is gravothermally stable and may be called a thermal system.

In the former case of the unlimited contraction, the final density profile is determined essentially by the density and temperature dependence of the heat conductivity. In the case of a system under the force of the inverse square law, the final density distribution is well approximated by a power law so that the mass contained in the condensed core is relatively small. A possibility of formation of a black hole in stellar systems is also discussed.

§ 1. Introduction

We shall discuss self-gravitating *gas systems* contained within a spherical adiabatic wall. When the temperature distribution is isothermal, the system is in thermal equilibrium in the sense that the variation of the total entropy of the system vanishes, i.e., $\delta S=0$. However, this system is gravothermally unstable, i.e., $\delta^2 S>0$, if the density contrast between the central density ρ_c and the density just inside the wall ρ_1 is greater than a certain critical value, i.e., $D=\rho_c/\rho_1>D_{\rm crit}=709$.[1)~4)] This instability is called the gravothermal catastrophe.

The gravothermal catastrophe develops as follows: As a result of fluctuation, heat is transported from an inner shell to an outer shell for example. The pressure in the inner shell decreases and this shell suffers from contraction because the system is self-gravitating. The increase of temperature by the adiabatic compression overcomes the decrease of temperature by the initial transport of heat. Then, the temperature gradient appears which helps transporting heat further. Because

of this instability, the central region of the system continues to contract as heat is transported outwards.

As far as the *gas system* is concerned, the existence of the gravothermal catastrophe has now been clearly shown within the scope of the linearized theories.[1)~4)] In particular, its physical significance was discussed in great detail by Hachisu and Sugimoto,[4)] which will be referred to as HS. In the present paper, we shall extend such studies into the non-linear regime of finite amplitude and seek what is the final fate of the catastrophe.

Though the gas system may behave differently from almost collision free stellar system, both of them may have common characteristics as a self-gravitating system. Since the gas system is easy to handle as compared with the stellar system, it will help clear understanding of physics involved in the catastrophe. Because the gravothermal catastrophe of finite amplitude is closely related with the gravitational contraction of an individual star, it will be treated in the same framework as the theory of stellar structure, for which we have already much better understanding.

In the next section we compute numerically the gravothermal catastrophe of the gas system up to a stage when the central density grows 10^{13} times its initial value. In § 3 we shall compute a couple of cases to see the effect of different choices of the coefficient of the heat transport. The mass of the centrally condensed core, which is formed as a result of the catastrophe, is found to be determined essentially by the functional form of the heat transport. In the final subsection a possibility for the formation of a black hole in the centrally condensed core of the stellar system will be discussed.

§ 2. Development of catastrophe in gas systems

2.1. *Basic equations*

In the present paper, we shall use the same notations as in HS. Equations appearing in HS will be denoted as Eq. (HS·3), for example. The basic equations for the present problem are the same as those for stellar structure in gravitational contraction. The equations of hydrostatic equilibrium, Eq. (HS·2) have to be supplemented by equations of the heat flow and of the energy conservation, i.e.,

$$\lambda \partial T/\partial r = -L_r/4\pi r^2 , \tag{1}$$

$$\partial L_r/\partial r = -4\pi r^2 \rho T (\partial s/\partial t)_{M_r} , \tag{2}$$

where L_r denotes the heat flux through the sphere of radius r, and t is the time. We assume that the heat conductivity λ is expressed as

$$\lambda = \lambda_0 \left(\frac{\rho}{M/4\pi R^3}\right)^{\alpha} \left(\frac{T}{GMm/kR}\right)^{\beta} . \tag{3}$$

For a while we choose $\alpha = 0$ and $\beta = 5/2$, which correspond to the heat conduc-

tivity of particles under the force of the inverse square law.

We shall use the non-dimensional variables for the Lagrangian mass coordinate ϕ, the radius x, the pressure p and the temperature θ as defined by Eq. (HS·6), the density ψ as defined by Eq. (HS·8), and the specific entropy σ as defined by Eq. (HS·9). Further, we define the non-dimensional heat flow and time as

$$f=L_r(GM^2/Rt_0)^{-1}, \tag{4}$$

$$\tau=t/t_0, \quad t_0\equiv\frac{kM}{4\pi\lambda_0 Rm}, \tag{5}$$

respectively. Then, the hydrostatic equilibria are described by Eq. (HS·7) and the thermal equations are rewritten as

$$\partial\theta/\partial x=-f/x^2\psi^\alpha\theta^\beta, \tag{6}$$

$$\partial f/\partial\phi=-\theta\partial\sigma/\partial\tau. \tag{7}$$

In addition to Eq. (HS·10), we have two further boundary conditions,

$$f=0 \text{ at } \phi=0 \text{ and } \phi=1. \tag{8}$$

2.2. *Initial models and procedures*

The isothermal gas spheres are characterized only by one parameter, the density contrast D. Their structures are conveniently expressed in Fig. 1, where the homology invariants are defined by

$$U\equiv\partial\ln M_r/\partial\ln r=x^3\psi/\phi, \tag{9}$$

$$V\equiv-\partial\ln P/\partial\ln r=\phi\psi/xp. \tag{10}$$

We may choose any point along the U-V curve as the outer boundary of the system, which will be denoted by the subscript 1. Then, the value of the density contrast is determined as indicated in Fig. 1.

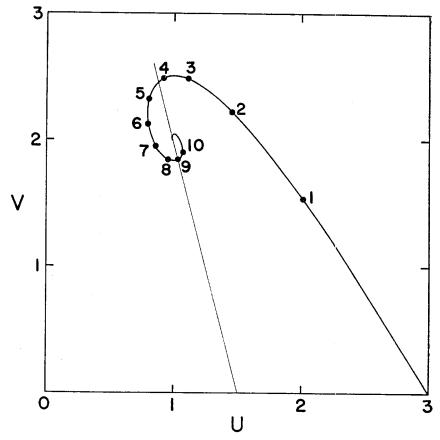

Fig. 1. U-V curve of the isothermal sphere. The thin straight line passes through the equi-energy points. Attached are the values of the density contrast in natural logarithm.

The total (thermal plus gravitational) energy of the isothermal gas sphere is computed easily from Eq. (HS·2) as

$$E_{\rm tot}=-\frac{GM^2}{R}\frac{1}{V_1}\left(\frac{3}{2}-U_1\right). \tag{11}$$

When the mass and the radius of the system are given, there are multiple solutions which have the same total energy. As shown in Fig. 1, the outer boundaries

of such solutions lie along a straight line which passes through the point $(U, V) = (3/2, 0)$.

Choosing a value of the density contrast, we obtain an initial isothermal model. Then, we impose initial ($\tau=0$) perturbation in entropy with the amplitude of $|\delta\sigma|_{\max}=0.08$, for which the linearized theory is still accurate enough. (If we started with a smaller amplitude, it would take additional time for the perturbation to grow up to our initial amplitude. The non-dimensional growth time is about 50.) Its dependence on the mass coordinate ϕ was taken from HS, i.e., from the eigenfunction of the fundamental mode which maximizes the variation in $\delta^2 S$ (see, e.g., Figs. 9 and 10 in HS). For this initial perturbation, we may choose two alternatives of its sign; one with $\delta\sigma_c<0$ (case A) and the other with $\delta\sigma_c>0$ (case B), where the subscript c refers to the value at the center. Then, the progress of the catastrophe was followed numerically by means of a Henyey-type program of stellar evolution.

2.3. *Numerical results*

When the initial density contrast is greater than $D_{\rm crit}$, the catastrophe commences as discussed in HS. Though we computed several cases of different initial conditions, we shall discuss only one case of the initial contrast of $D_0=8100$, since essential features are the same for every D_0 greater than $D_{\rm crit}$. The changes in the density and the temperature profiles are shown in Figs. 2(a) and 2(b), respectively, both for the cases A and B of the initial perturbations.

We shall discuss the case A in the first place. As seen in Fig. 2(b), the minimum of the temperature lies around $x\simeq 0.04$, i.e., $\phi\simeq 0.06$. The heat flows toward this point from both sides. As the heat flows out of the central region, the core contracts gravitationally as seen in Fig. 2(a). The contraction of Lagrangian shells is shown in Fig. 3. As seen both in Figs. 2(a) and 3, it results in a strong central condensation developing a strong core-halo structure. For our amplitude of the initial perturbation, the time scale of contraction is about 100 t_0, where t_0 is of the order of the Kelvin time scale for the initial stage [see Eq. (5)]. The change in the internal structure is seen also in the U-V plane of Fig. 4. The U-V curve grows to make a big loop above that of the isothermal core, which implies a strong cen-

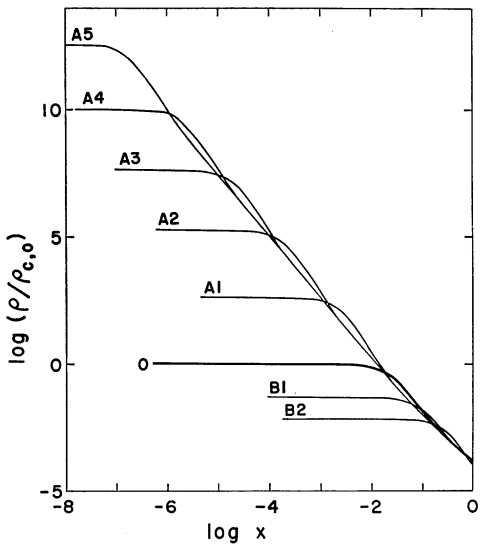

Fig. 2(a).

(Figure caption is printed on the next page.)

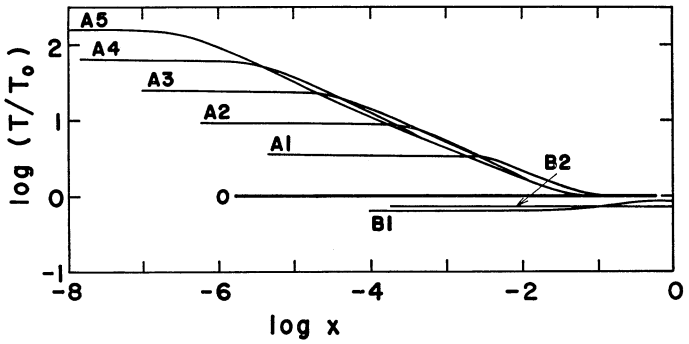

Fig. 2(b).

Fig. 2. Density (Fig. 2(a)) and temperature (Fig. 2(b)) profiles shown against the non-dimensional radial coordinate. In the ordinates the density is normalized by the central density in the initial stage $\rho_{c,0}$ and the temperature by the initial (isothermal) temperature T_0. The thick curve labelled with 0 is the initial model which is common to both cases A and B. Attached are the stage numbers A1 through A5 for the evolution in the case A, and B1 through B2 for the case B. The non-dimensional times of evolution are $\tau=0.0$(0), 130.41 (A1), 137.15(A2), 138.72 (A3), 139.12(A4) and 139.21(A5), and 101.16(B1) and 445.57(B2).

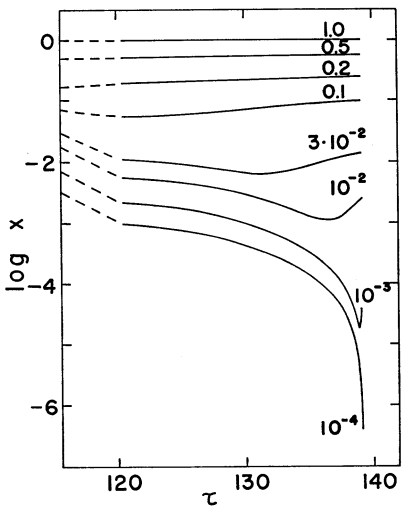

Fig. 3. Time variation of the radial distances of Lagrangian shells. The left ends of the dashed lines correspond to the initial isothermal configuration. Attached are the mass coordinates ϕ of the Lagrangian shells.

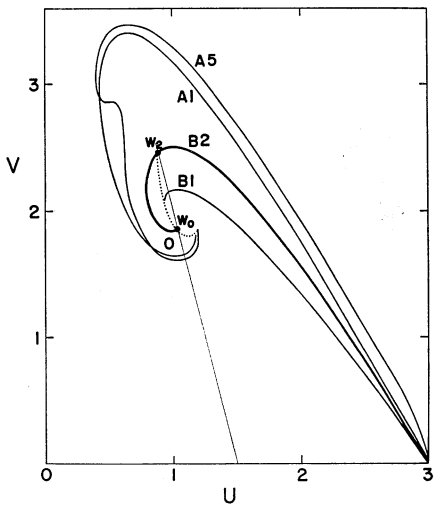

Fig. 4. Changes in U-V curves for the cases A and B. The thick solid curve represents the isothermal configuration. The U-V curve for the initial stage extends up to the point W_0. The U-V curve for the stage B2 practically overlaps it, but extends up to the point W_2. The dotted curves show the change in the point of the outer boundary of the system.

tral condensation and a temperature gradient decreasing outward in the central region.

The total entropy of the system S continues to increase at the rate of

$$\frac{dS}{dt}=\int_0^M\left(\frac{\partial s}{\partial t}\right)_{M_r}dM_r=\int_0^M\frac{L_r}{4\pi r^2}\frac{\partial}{\partial r}\left(\frac{1}{T}\right)\frac{1}{\rho}dM_r\,. \tag{12}$$

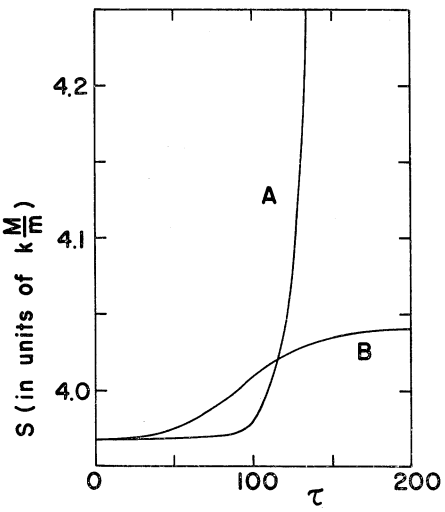

Fig. 5. Changes in the total entropy of the system for the cases A and B.

Though Eqs. (1) and (2) were used to obtain the extreme right-hand side of Eq. (12), it may be written down directly according to the thermodynamics of irreversible process, since entropy is being produced by the heat conduction as an irreversible process. In the case A, the total entropy of the system continues to increase as shown in Fig. 5, and the system remains to be a gravothermal system in the sense that the density contrast remains greater than $D_{\rm crit}$.

In the next place, we shall discuss the case B of the initial perturbation. The result of computation is already shown in Figs. 2(a), 2(b) and 4. In this case, the temperature is decreasing inward in the central region. As the heat flows into the central region, the core expands against the self-gravity. Then the temperature in the central region decreases further, because the tensor specific heat thereof is negative as discussed in HS. As the central region expands, the density contrast D is reduced as seen in Fig. 2(a). Therefore, the system becomes less gravothermally unstable.

Near the stage B1, the central temperature turns to increase, which implies that the tensor specific heat turns positive. Afterwards, the system approaches another isothermal configuration as seen in Figs. 2(b) and 4. This configuration corresponds to the U-V curve in Fig. 4 which ends at the equi-energy point W_2. Its total energy is the same as the initial model but its density contrast is smaller than $D_{\rm crit}$. It is gravothermally stable and was called a thermal system in HS. During the transition from the initial gravothermal system to the final thermal system, the total entropy of the system increases at the rate of Eq. (12), and finally leveles off to its local maximum value ($\partial^2 S<0$) as seen in Fig. 5.

§ 3. Discussion

3.1. *Density profile produced by the catastrophe*

We shall compare our results with other treatment of the stellar dynamics.

As for the gravitational N body problem, available computations cover the contraction only by a factor of about 100 in the central density,[5)~7)] when it is seen with a coarse grain containing at least three particles (i.e., excluding the case of only one binary). On the other hand, Larson[8)] computed up to a stage of the central density 10^8 times the initial value by his fluid dynamical approach. He made the Fokker-Planck approximation of the Boltzmann equation to treat the almost collision free system, in which the moments of the velocity distribution were taken up to fourth order. Larson's approach is intermediate between ours and the gravitational N body problem, since the distribution function is described in μ-space but the mechanism of energy transport is essentially different from our diffusion approximation.[8)]

The density profile, which is produced as a result of the catastrophe, is shown in Fig. 1 of Larson's paper.[8)] Simulation of the N body problem by means of the Monte Carlo method[9)] gave a result similar to Larson's in its essential feature. Here we shall compare our density profile in Fig. 2(a) with Larson's.[8)] It is found that both of them are in excellent agreement, which are well approximated by

$$\rho \propto r^{-2.4}, \tag{13}$$

except for the very central region.

The density profile as appeared in Eq. (13), the power index in particular is interpreted as follows. Let us assume that the density distribution is expressed by the power law,

$$\rho \propto r^{-\nu}. \tag{14}$$

From Eq. (HS·2) and the equation of state we obtain

$$M_r \propto r^{3-\nu}, \quad T \propto r^{2-\nu}. \tag{15}$$

From Eqs. (1)$\sim$(3), (14) and (15), we obtain

$$t_r \propto r^{2-2\beta-\nu(1-\beta-\alpha)}, \tag{16}$$

for the local time scale of heat transport. This implies that the heat transport is more rapid in the inner shell for the case of $(\alpha, \beta) = (0, 5/2)$. As seen in Fig. 3, the local time scale of a given Lagrangian shell decreases more and more as the contraction proceeds. Therefore, the central core contracts more and more rapidly with the relatively outer halo left behind, which results in the smaller and smaller core mass.

As imagined from Eq. (16), the final density profile will depend upon the power indices (α, β) of the conductivity. In order to see its dependence, we computed a couple of artificial cases with different sets of (α, β). It is found that the density profile is determined mainly by the value of α though it is difficult to

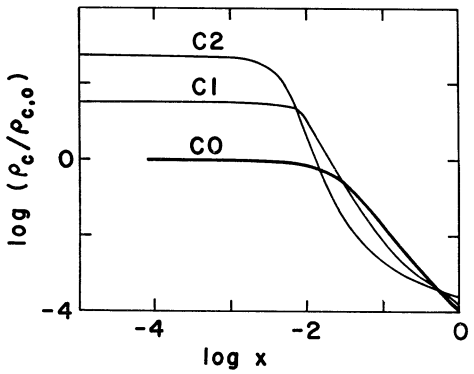

Fig. 6. The same as Fig. 2(a) but for the case of $(\alpha, \beta) = (0, -1)$. The non-dimensional time of evolution is 0(C0), 240(C1) and 720 (C2).

give a clear-cut description. For moderate values of β, positive α yields the density profile well approximated by Eq. (14) with the index ν between 2.0 and 2.5.

On the other hand, negative and vanishing value of α yields a reatively large core. Figure 6 shows the case of $(\alpha, \beta) = (0, -1)$, where the power law of Eq. (14) is no longer a good approximation. In this case, the time scale of heat transport is longer in the inner shell.

3.2. *Gravitational energy*

The total gravitational energy of the system is expressed as

$$\Omega = \omega(R, 0), \quad \omega(r_b, r_a) = -\int_{r_a}^{r_b} \frac{GM_r}{r} dM_r . \tag{17}$$

In Fig. 7, the non-dimensional gravitational energies Ω/Ω_0 are shown against the central density, where $\Omega_0 (<0)$ is the initial gravitational energy. For the case of $(\alpha, \beta) = (0, 5/2)$, its absolute value increases first and then turns to decrease.

As we did in the preceding subsection, we shall approximate the density profile by Eq. (14) for the region of $r > r_a$. Then, Eq. (17) gives

$$-\omega(r_b, r_a) \propto \frac{3-\nu}{5-2\nu} ({r_b}^{5-2\nu} - {r_a}^{5-2\nu}) . \tag{18}$$

For $\nu < 5/2$, the total gravitational energy is determined mainly by the halo in the

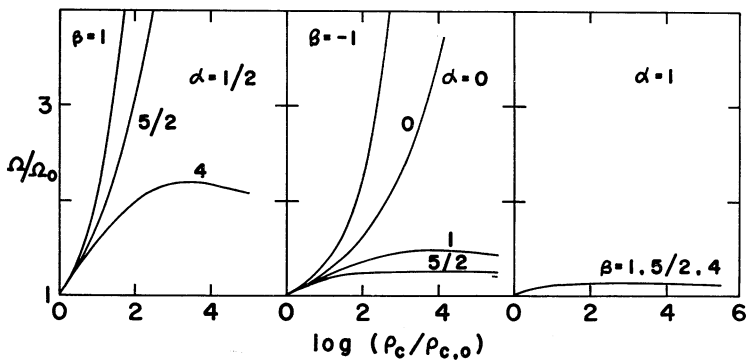

Fig. 7. Changes in the gravitational energy with the progress of the catastrophe. Cases for different sets of (α, β) are shown as indicated in the Figure.

limit of infinitely high central density, or in other words $r_a \to 0$ as seen in Fig. 2(a). Thus in our case of Eq. (13) the gravitational energy is not released indefinitely, though the central density increases indefinitely. The reason is also seen in Fig. 3: A Lagrangian shell, which has been contracting, turns into expansion at a certain stage. In such cases the density profile of the power law is realized.

On the contrary, the gravitational energy is released indefinitely when α and β are small, as seen in Fig. 7. According to the theory of internal constitution of the stars, the gravitational contraction of a star is understood also in terms of the gravothermal catastrophe.[4] In this case the law of the heat conductivity is different from one considered above. Thus, a relatively large core is formed and the gravitational energy is determined mainly by the core.

3.3. *Formation of a black hole*

For a Lagrangian shell inside the system, the ratio of its *local gravitational radius* r_g to its local radius is given by

$$\frac{r_g}{r}=\frac{2GM_r}{c^2 r}=\frac{2GM}{Rc^2}\frac{\phi}{x}\propto\left[\frac{3}{3-\nu}r^{2-\nu}-\frac{\nu}{3-\nu}r_a{}^{3-\nu}r^{-1}\right], \tag{19}$$

where the density is assumed to be constant in the region of $r<r_a$. When ν is greater than 2 as in our case, there is a possibility of the formation of a black hole. As seen in Fig. 3, a Lagrangian shell contracts in the first place and then turns to expand. We define the contracting part as the core, which will be denoted by the subscript core. Figure 8 shows $(\phi/x)_{\text{core}}$ against the non-dimensional mass of the core ϕ_{core} which is decreasing in time. If $(\phi/x)_{\text{core}}$ exceeds $Rc^2/2GM$, a black hole of mass $M\phi_{\text{core}}$ is regarded to be formed as a result of the catastrophe. These results are applied to typical objects as listed in Table I, though there remains some doubt against its validity in the case of collisionless stellar systems.

In most systems the mass of the black hole is too small to be considered as created by the gravothermal catastrophe, because the core mass is too small in the case of $(\alpha, \beta)=(0, 5/2)$, i.e., in the case of the system under the force of the

Table I. Formation of a black hole.*)

	R(pc)	$M/M_\odot$	$Rc^2/2GM$	$M\phi_c/M_\odot$	t_d(yr)	t_c(yr)
globular cluster	10	10^5	10^9	$\ll 1$	$10^{9.4}$	10^{18}
elliptical galaxy	$2\cdot10^4$	10^{11}	$2\cdot10^6$	10	$10^{17.4}$	$10^{20.5}$
compact galaxy	10^3	10^{11}	10^5	10^3	$10^{15.5}$	10^{16}
semi-stellar nucleus of QSO	1	10^9	10^4	300	$10^{9.8}$	10^{10}

*) Here, R is the initial radius of the stellar system, $M\phi_c$ is the mass of the core when its radius has shrunk down to its local gravitational radius, t_d is the time scale of the dynamical friction,[8] and t_c is the time scale of the direct star-star collision. Parameters of the heat conductivity are assumed to be $(\alpha, \beta)=(0, 5/2)$.

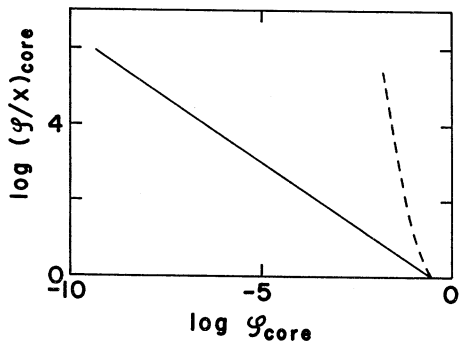

Fig. 8. Ratio of the non-dimensional mass ϕ and the radius x at the edge of the contracting core. The non-dimensional core mass decreases as the catastrophe proceeds. The solid curve is for the case of $(\alpha, \beta) = (0, 5/2)$ and the dashed curve is for $(0, -1)$.

inverse square law. In very compact and massive systems as represented by a compact galaxy and a semi-stellar nucleus of quasi-stellar object, however, the mass of the black hole may be marginally large. In the formation of a black hole various processes may be involved which have not been considered in the present paper. Among them are direct star-star collisions which disrupt the stars. However, the most important is the mechanism of heat transport in a real stellar system, which determines the mass of the core as examplified in Fig. 8 by the artificial case of $(\alpha, \beta) = (0, -1)$. In this sense detailed studies on the transport mechanism in almost collision free stellar systems are most desirable to clarify their difference, if any, from the gas system.

Acknowledgements

The authors would like to thank Professor M. Miyamoto for discussions. Numerical computations were made at the Computer Center of the University of Tokyo.

References

1) V. A. Antonov, Vest. leningr. gos. univ. **7** (1962), 135.
2) D. Lynden-Bell and R. Wood, Month. Notices Roy. Astron. Soc. **138** (1968), 495.
3) Y. Nakada, Publ. Astron. Soc. Japan **30** (1978), 57.
4) I. Hachisu and D. Sugimoto, Prog. Theor. Phys. **60** (1978), 123.
5) S. J. Aarseth, M. Hénnon and R. Wielen, Astron. and Astrophys. **37** (1974), 183.
6) S. J. Aarseth, Vistas in Astronomy **15** (1973), 13.
7) S. J. Aarseth, Astron. and Astrophys. **35** (1974), 237.
8) R. B. Larson, Month. Notices Roy. Astron. Soc. **147** (1970), 323.
9) M. Hénon, Astrophys. Space Sci. **13** (1971), 284.